

Measurement of Mass-Transfer Rates for Surfactant-Enhanced Solubilization of Nonaqueous Phase Liquids

ALEX S. MAYER* AND LIRONG ZHONG

Department of Geological Engineering and Sciences, Michigan Technological University, Houghton, Michigan 49931-1295

GARY A. POPE

Center for Petroleum and Geosystems Engineering, University of Texas, Austin, Texas 78712

Surfactant-enhanced solubilization of residual, non-aqueous-phase liquid (NAPL) contaminants is an emerging, subsurface remediation technology. The potential for nonequilibrium conditions is investigated for surfactant-enhanced solubilization of a NAPL, trichloroethylene (TCE), in a model porous medium. The surfactant formulation consists of an anionic surfactant, sodium dihexyl sulfosuccinate, an alcohol, and an electrolyte in aqueous solution. Batch solubilization experiments are conducted to assess the significance of chemical rate limitations. Surfactant flood experiments are conducted in packed columns with residual TCE. Mass-transfer rate coefficients are determined as a function of aqueous-phase pore velocity, NAPL volumetric fraction, and surfactant concentration. A correlation for predicting mass-transfer rate coefficients as a function of system properties is developed. The mass-transfer rate coefficients and correlation are obtained by fitting a transport simulator to the column effluent concentration results. Significant differences are found between the correlation developed here and correlations developed for other NAPL–surfactant systems. The correlation predicts near-linear dependences of mass-transfer rates on the NAPL volumetric fraction and pore velocity. Using the Damkohler number, the degree of nonequilibrium behavior in surfactant-enhanced NAPL solubilization is analyzed for a range of conditions. Nonequilibrium conditions are found to be significant at relatively low NAPL volumetric fractions.

1. Introduction

Surfactant flooding is an emerging technology for remediating aquifers contaminated with nonaqueous phase liquids (NAPLs). Surfactant flooding involves the injection of a chemical surfactant solution through zones of the subsurface contaminated by NAPLs. Upon contact with the NAPL, the surfactant produces an apparent increase in the aqueous solubility of the NAPL constituents. The solubility increase accelerates the rate of dissolution into the groundwater, when compared to the rate encountered when flooding with

freshwater alone, as in pump-and-treat systems. Surfactant flooding also can produce mobilization of the NAPL, as a pure phase, rather than or in addition to solubilization in the groundwater.

In the present work, we are considering solubility enhancement alone. Enhanced solubilization occurs via the partitioning of NAPL molecules into surfactant micelles, assuming that the surfactant concentration is above the critical micelle concentration (cmc). Most approaches to modeling enhanced solubilization assume that solubilization is a local equilibrium process. However, little work has been conducted to investigate whether nonequilibrium behavior can be significant. Furthermore, the physical and chemical conditions producing nonequilibrium behavior are not well understood, and reliable, quantitative models for predicting solubilization rates are not available. A better understanding of the nonequilibrium behavior in NAPL–surfactant systems is important for predicting and designing surfactant remediation systems.

The occurrence of nonequilibrium in surfactant-enhanced solubilization has been investigated in laboratory and field experiments. Pennell et al. (1) observed rate-limited solubilization in column experiments with a dodecane–polyoxyethylene (POE)–sorbitan monooleate system. They observed dodecane concentrations in the column effluent that were lower than the equilibrium values, increases in effluent concentrations following flow interruptions, and reductions in effluent concentrations when pore velocities were increased. Similar observations were reported by Pennell et al. (2) for perchloroethylene (PCE)–sodium sulfosuccinate systems. Abriola et al. (3) developed a correlation for estimating mass-transfer rate coefficients as a function of system properties for the dodecane–polyoxyethylene (POE)–sorbitan monooleate system. Mason and Kueper (4) conducted column experiments where pooled PCE was solubilized using a mixture of a nonylphenol ethoxylate and a phosphate ester of a nonylphenol ethoxylate surfactant. Near-equilibrium concentrations were observed in the first tens of pore volumes, followed by a gradual tailing toward lower concentrations. Decreases in pore velocities were found to produce higher solubilization efficiencies. Ji and Brusseau (5) reported tailing behavior in column experiments conducted with trichloroethylene (TCE) and sodium dodecyl sulfate.

Tailing behavior was found in a field experiment conducted by Fountain et al. (6). The NAPL–surfactant system consisted of PCE and a mixture of a nonylphenol ethoxylate and a phosphate ester of a nonylphenol ethoxylate surfactant. The field experiment involved the solubilization of residual and pooled PCE in a test cell installed in a sandy aquifer. Increases in effluent concentrations also were observed after a prolonged shutdown. However, it is not clear whether these observations of nonequilibrium behavior were due to rate-limited solubilization or to physical phenomena, such as heterogeneous distributions of NAPLs and aqueous-phase pore velocities.

A conceptual model suggested for describing rate-limited dissolution of NAPLs into freshwater involves diffusion of NAPL molecules from the NAPL–aqueous phase interface into the bulk, flowing aqueous phase (e.g., 7). The concentration at the NAPL–aqueous phase interface is assumed to be at equilibrium, such that this model can be described mathematically as

$$\frac{d(\theta_n \rho_n)}{dt} = k(C_s - C) = k_a(C_s - C) \quad (1)$$

* Corresponding author, Department of Geological Engineering and Sciences, 1400 Townsend Drive, Michigan Technological University, Houghton, MI 49931. Phone: (906) 487-3372; fax: (906) 487-3371; e-mail: asmayer@mtu.edu.

where θ_n and θ_w are the NAPL and water volumetric fractions, respectively (liquid volume/bulk volume); ρ_n is the NAPL density; C is the aqueous-phase concentration; k is the mass-transfer rate coefficient; C_s is the aqueous-phase solubility or equilibrium concentration; k_l is the mass-transfer coefficient; and a is the specific interfacial area between the NAPL and aqueous phase. The simplest, equivalent conceptual model for surfactant-enhanced solubilization would involve diffusion of the NAPL molecule from the interface into the bulk, flowing aqueous phase, where the NAPL molecule is incorporated into a surfactant micelle.

However, Carroll (8) and Ward (9) have suggested that the micelles must first diffuse to the NAPL–aqueous phase interface, disassociate into surfactant monomers, and adsorb at the interface. These steps are followed by incorporation of NAPL molecules into the surfactant monomers, reformation and desorption of the micelles from the interface, and diffusion of the micelles away from the interface. Diffusion of the micelles would take place in the hydrodynamic boundary layer. Any of these diffusion or sorption–desorption steps could be rate limiting. Carroll (8) found that the adsorption of the micelle at the interface was the rate-limiting step for highly insoluble oils in nonionic surfactant solutions. Chen et al. (10) suggested that, if the adsorption rate of micelles on the interface was rate limiting, the mass-transfer rate should be proportional to surfactant concentration. On the other hand, Grimberg et al. (11) suggested that diffusion of micelles away from the interface was rate limiting for solubilization of phenanthrene into a nonionic surfactant solution. The model of Grimberg et al. (11) for estimating the overall mass-transfer coefficient indicated that the mass-transfer rate decreases with increasing surfactant concentration.

An alternative explanation for observations of nonequilibrium behavior in the freshwater dissolution of NAPLs is physical nonequilibrium, or bypassing (12). In this situation, the aqueous phase is flowing through a combination of regions containing NAPL and regions with no or very little NAPL present. The aqueous phase in the regions containing NAPL would be at or near equilibrium concentrations, whereas the aqueous concentrations in the regions without NAPL would be nearly zero. Thus, the observed average concentration over all of the regions would be lower than the equilibrium concentration. The same concept could be applied to surfactant-enhanced solubilization. The significance of physical nonequilibrium was explored by Pennell et al. (1) in their study of surfactant-enhanced solubilization experiments. However, they suggested that the rate limitations observed in their column experiments could not be attributed to physical nonequilibrium. This conclusion was based on tracer test results, which implied that the aqueous phase was flowing through regions with uniform NAPL volumetric fractions.

In this work, we are hypothesizing that a linear driving force approach described in eq 1 is valid for describing observations of nonequilibrium, surfactant-enhanced solubilization, and we test this hypothesis with new experimental data. We focus on a surfactant formulation that has been shown to perform well for solubilizing a specific NAPL, TCE (13). We measure mass-transfer rate coefficients and investigate the dependence of the rate coefficients on system properties such as aqueous-phase pore velocity, NAPL volumetric fraction, and surfactant concentration. We develop a correlation for estimating mass-transfer rate coefficients as a function of system properties and compare the correlation with correlations developed for other NAPL–surfactant systems. Last, we use the correlation to analyze the sensitivity of the degree of nonequilibrium to the estimated parameters and system properties.

2. Materials and Methods

2.1. Overview. Experiments were conducted to determine the rate of mass-transfer in NAPL–aqueous surfactant systems. Batch experiments were conducted under completely mixed conditions to assess the significance of rate limitations as a result of NAPL–surfactant chemical interactions, such as micelle formation, microemulsion coalescence, or sorption–desorption of micelles from the NAPL–aqueous interface, for two different surfactant concentrations. A series of column experiments was conducted at various aqueous pore velocities and with two different surfactant concentrations. The purpose of the column experiments was to allow quantification of mass-transfer rates as a function of pore velocity, NAPL volumetric fraction, and surfactant concentration. A transport model was developed to estimate parameters from the column effluent data.

2.2. Materials. The surfactant formulation consisted of an aqueous solution of 1.6% (all percentages are given as the weight of active compound/weight of solution) or 4.0% sodium dihexyl sulfosuccinate surfactant (purchased as Aerosol MA with an 80% active surfactant concentration, Cytec Inc., West Paterson, NJ), 4.0% 2-propanol (IPA, reagent grade, Aldrich Chemical Co., Milwaukee, WI), and 3000 ppm sodium chloride. Since sodium dihexyl sulfosuccinate is an anionic surfactant, its solubilization properties are controlled by electrolyte concentrations, among other physical and chemical conditions. IPA is added to reduce the potential of the formation of liquid crystals in the aqueous phase due to NAPL–surfactant interactions (14). Each of the surfactant concentrations is significantly higher than the cmc. The NAPL used in the experiments was TCE (Aldrich Chemical Co.), which is a commonly found groundwater contaminant. TCE has a density of 1.46 g/cm³ and an aqueous solubility of 1100 mg/L. The water used in the experiments was distilled and deionized. Interfacial tensions of TCE against the 1.6% and 4.0% surfactant solutions were measured as 0.68 ± 0.09 and 0.44 ± 0.06 dyn/cm at 15 °C, respectively, with a Kruss SITE 04 spinning drop tensiometer (Kruss USA, Charlotte, NC). Viscosities of the 1.6% and 4.0% surfactant solutions were measured at 15 °C as 1.63 and 1.82 cP, respectively, with a Contraves LS-30 Couette viscometer (Contraves, Inc., Bern, Switzerland). Densities of the 1.6% and 4.0% surfactant solutions at 15 °C were calculated as 1.02 and 1.03 g/cm³, respectively, using an apparent density method described in Kostarelos et al. (15). The porous media was a 40–70-mesh (grain size range from 0.211 to 0.419 mm; geometric mean grain size of 0.282 mm) Ottawa sand (U.S. Silica, Ottawa, IL).

2.3. Batch Test Procedures. Batch solubilization experiments were conducted under constant-temperature conditions, at a temperature of 15 ± 0.3 °C. Borosilicate glass vials with Teflon-lined septa were filled with approximately equal volumes of TCE and surfactant solution. The vials were placed in a tumbler and tumbled at a 15 rpm rotational speed. The vials were taken from the tumbler periodically for sampling. Before sampling, the TCE and aqueous-phase mixtures were centrifuged at 7000 rpm for 30 min, to separate any droplets of TCE as NAPL from the aqueous phase. The centrifugate was withdrawn with a gastight syringe and injected in a vial containing a known amount of water for dilution purposes. Diluted samples were then analyzed for TCE concentrations with a Shimadzu gas chromatograph (Columbia, MD) equipped with a flame ionization detector, where the detection limit for TCE was approximately 5 mg/L.

2.4. Column Test Procedures. The experimental columns consisted of a 2.54-cm inside diameter stainless steel tube with stainless steel endcaps. The endcaps were fitted with 150-mesh stainless steel screens. The column length was either 5 or 13 cm. The column was packed with dry porous media. Measured porosities were an average of 0.358 with

a standard deviation of 0.007. After packing, the column was flushed with CO₂ followed by saturation with deaired water. The column was then flooded with TCE, using either a pump (Fluid Metering Inc., FMI, Oyster Bay, NY) or a pressurized water-drive system. Once water was no longer observed in the effluent, the TCE flood was terminated. Next, the column was flooded with deaired water to produce residual TCE in the column. The water flood was conducted with either a pump or a pressurized water-drive technique. The water flood was terminated when TCE was no longer observed in the column effluent.

The surfactant flood was conducted by pumping surfactant solution from a glass reservoir to the column influent with the FMI pump. The surfactant floods were conducted in a downflow mode. During surfactant floods, the column was submerged in a constant-temperature water bath, which was maintained at a temperature of 15 ± 0.3 °C. Constant pumping rates were used with the exception of a few flow-interruption experiments. Aqueous samples were collected from the column effluent by directing the effluent tubing through Teflon-lined septa and into borosilicate, 20-mL glass vials. The sample vials were prefilled with water, and the end of the effluent tubing was held below the water in the vials to prevent contact of the effluent with air and minimize volatilization losses. Standard solutions of TCE were subjected to the same procedures as the effluent samples; losses during sampling were found to be less than 1%. The effluent tubing was 0.32-cm nominal diameter stainless steel. The column experiments proceeded until between 50% and nearly 100% of the TCE had been solubilized. The effluent concentrations at the end of the experiments where nearly 100% of the TCE was solubilized were typically on the order of 20 mg/L; the lowest TCE concentration measured was 14 mg/L.

The initial and final NAPL volumetric fractions were measured in all of the experiments by weighing the column before and after the surfactant flood. In addition, the initial NAPL volumetric fractions were measured with a partitioning tracer test (16) in the first five column experiments. The average difference in measured volumetric fractions between the gravimetric and partitioning tests was 3%. Mass balances were estimated by integrating the effluent concentration vs pore volumes curves and comparing the solubilized mass to the difference in the measured initial and final volumetric fractions. The difference between masses estimated from the effluent data and volumetric saturation measurements was on the order of 7%.

2.5. Modeling and Parameter Estimation. A transport simulator was developed by applying second-order centered finite-difference approximations in space and an implicit Euler approximation in time to the following one-dimensional advective-dispersive equation for aqueous-phase transport (2) and the mass balance equation for NAPL solubilization (1):

$$\frac{\partial(\theta_w C)}{\partial t} = -q \frac{\partial C}{\partial x} + \theta_w D \frac{\partial^2 C}{\partial x^2} + k(C_s - C) \quad (2)$$

where $q = v\theta_w$ is the aqueous-phase Darcy velocity, v is the aqueous-phase pore velocity, $D = \alpha_L v + \tau D^*$ is the aqueous-phase dispersion coefficient, α_L is the longitudinal dispersivity, τ is the tortuosity, and D^* is the free liquid diffusion coefficient. In each time step, eq 2 was solved first, followed by solution of eq 1; the equations were solved iteratively until θ_n and C converged to a specified error criterion. The simulator was benchmarked against an analytical solution to the transient, advective-dispersive-reactive equation, and excellent agreement was found. Mass balance errors for all simulations were less than 1%. Temporal and spatial discretizations were set such that typical Courant number ($Cr = v\Delta t/\Delta x \leq 1$) and Peclet number ($Pe = v\Delta x/D \leq 2$)

constraints for second-order finite-difference approximations in space and implicit approximations in time were not violated. Grid convergence studies were performed to ensure that the parameter estimates did not depend on time step or spatial discretization sizes, given that the mass-transfer rate coefficients were relatively high.

Correlations for relating the mass-transfer rates to system properties have been developed for dissolution and solubilization in NAPL-freshwater, NAPL-cosolvent, and NAPL-surfactant systems (e.g., 7, 17, 18, 4). These correlations typically take a form similar to

$$Sh = \beta_0 Re^{\beta_1} \theta_n^{\beta_2} \quad (3)$$

where $Sh = kd_p^2/D^*$ is the modified Sherwood number, d_p is the particle size, $Re = v\theta_w d_p/\mu$ is the Reynolds number, ρ is the aqueous-phase density, μ is the aqueous-phase dynamic viscosity, and β_i are fitted parameters. A mass-transfer correlation of the form shown in eq 3 was incorporated into the transport simulator.

The column effluent data from each experiment were fitted with the simulator by varying the β_i parameters in eq 3 until a best fit was obtained. All other variables in eqs 1–3 were independently determined by experimental conditions. The parameter β_0 and the dimensionless number Re were assumed to be constant over the duration of an experiment, such that each individual experiment produced an independent estimate of β_2 , the exponent on the NAPL volumetric fraction. The value of β_0 also was fitted for each experiment. Finally, the value of β_1 was fitted to the ensemble of experimental results.

The goodness of fit was measured with a sum of the squares normalized residual, expressed as

$$\bar{r}^2 = \sum_{i=1}^n \left[\frac{C_{obs} - C_{sim}}{C_{obs}} \right]^2 \quad (4)$$

where C_{obs} is the observed effluent concentration and C_{sim} is the simulated effluent concentration. The confidence intervals for the parameter β_2 were estimated for each experiment using the jackknife method described by Efron and Gong (19). Confidence intervals for the other two parameters were obtained over all experiments by conventional t-test methods (20).

3. Results and Discussion

3.1. Batch Experiments. Parts a and b of Figure 1 show the results from batch experiments with 1.6% and 4.0% surfactant concentrations. The equilibrium TCE concentrations for the 1.6% and 4.0% surfactant concentrations were 6100 and 31 300 mg/L, respectively. The results in Figure 1a show that equilibrium concentrations are attained within a few minutes under well-mixed conditions. The relatively quick attainment of equilibrium conditions indicates that processes such as micelle formation or sorption-desorption of micelles from NAPL-aqueous interfaces may not be rate limiting for this NAPL-surfactant system. The batch experiment results were fitted with a first-order rate model, $dC/dt = -k_b(C_s - C)$, where k_b is the first-order rate constant. The resulting model fits are shown in Figure 1b, where the fitted k_b for the 1.6% and 4.0% surfactant concentrations were 2.4 and 1.5 min⁻¹, respectively. The R^2 values of the log-transformed fits of the 1.6% and 4.0% surfactant concentrations were 0.986 and 0.953, respectively. The higher rate constant for the lower surfactant concentration may be explained by the fact that the ratio of micelles to moles of alcohol decreases as the surfactant concentration increases, since the alcohol concentration remained almost constant for both surfactant solutions. Alcohols such as IPA are known to increase

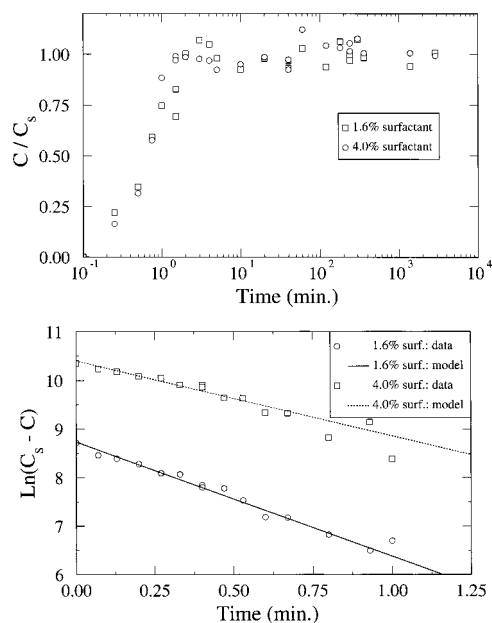


FIGURE 1. (a, top) Batch experiment results for two surfactant concentrations. Concentrations normalized by equilibrium concentrations are plotted with respect to sampling time. (b, bottom) Fitting of batch experiment results for two surfactant concentrations with a first-order rate model.

TABLE 1. Experimental Conditions and Estimated Model Parameters

surfactant concn, %	init NAPL vol fraction, %	av pore velocity, cm/s	mass-transfer model parameter	
			β_0	β_2^a
1.6	2.3	0.014	940	1.15 ± 0.03
1.6	2.8	0.014	820	1.14 ± 0.05
1.6	3.0	0.014	820	1.16 ± 0.06
1.6	3.1	0.014	820	1.14 ± 0.05
1.6	3.8	0.015	790	1.13 ± 0.04
1.6	3.8	0.015	530	1.12 ± 0.06
1.6	4.0	0.015	620	1.12 ± 0.02
4.0	2.1	0.0059	410	1.21 ± 0.07
4.0	3.3	0.012	360	1.18 ± 0.07
4.0	2.8	0.013	380	1.12 ± 0.04
4.0	3.3	0.021	400	1.12 ± 0.03
4.0	2.5	0.0077	350	1.12 ± 0.04

^a Estimated value \pm 95% confidence interval.

coalescence times for microemulsions, such that a decrease in the ratio of micelles to moles of alcohol could result in a decrease in NAPL-surfactant reaction rates (14).

3.2. Column Experiments, Mass-Transfer Rates, and Parameter Estimates. Table 1 lists the experimental conditions for each of the column experiments where constant influent flow rates were applied. A typical result from a column experiment is shown in Figure 2, where effluent concentrations are plotted against pore volumes flooded. Equilibrium is observed within about a pore volume of surfactant flood, in coincidence with breakthrough of the surfactant. Equilibrium concentrations are maintained for several more pore volumes, until about 25% of the NAPL has been solubilized. At this point, the effluent concentrations decrease steadily below equilibrium levels for several more pore volumes. Eventually, tailing is observed, where concentrations are far below equilibrium levels and decrease slowly.

Three other experiments were conducted where the influent flow was interrupted for 44–72 h and then resumed

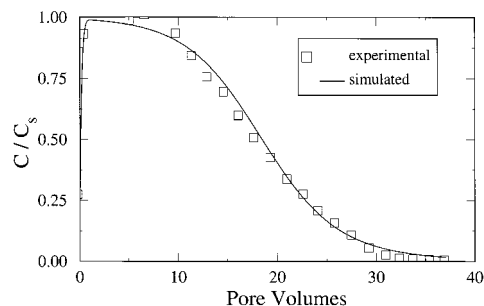


FIGURE 2. Column experiment results (symbols) for 1.6% surfactant concentration, pore velocity = 0.014 cm/s, initial NAPL volumetric fraction = 8.7%, and best-fit model simulation (line). Concentrations normalized by equilibrium concentrations are plotted with respect to pore volumes flooded through the column.

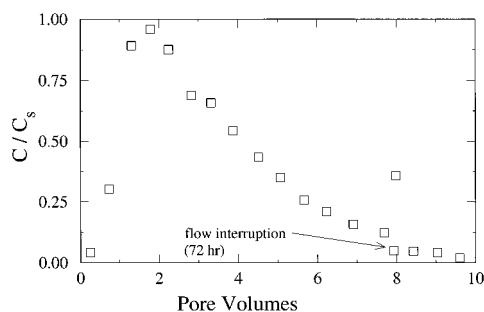


FIGURE 3. Column experiment results for 4.0% surfactant concentration, pore velocity = 0.011 cm/s, initial NAPL volumetric fraction = 7.8%, and a flow interruption period of 72 h. Concentrations normalized by equilibrium concentrations are plotted with respect to pore volumes flooded through the column.

at the previous flow rate. In each case, the effluent concentrations following resumption of flow were significantly higher than the concentrations preceding flow interruption. This result indicates that the system was out of equilibrium before the flow interruption. Figure 3 shows the results of a flow-interruption experiment, where the pore velocity during flooding was 0.011 cm/s and the flow-interruption period was 72 h. At the beginning of the flow interruption, the TCE volumetric fraction was approximately 2.7%, which would provide a sufficient mass to produce equilibrium concentrations in the pore water, if enough time were allowed. However, when the flow was resumed after 72 h of interruption, concentrations far below equilibrium are observed. This result indicates that the system was out of equilibrium at the beginning of the flow interruption and that diffusion rates in the stagnant pore water are low.

Sorption of TCE onto the porous media is not expected to affect the observed effluent concentrations. First, the porous medium used in the experiments contains no measurable organic carbon (Ottawa sand), and second, little or none of the surfactant will sorb to the porous medium, due to its anionic character. Dwarakanath et al. (26) measured a distribution coefficient of 0.0017 for the same surfactant formulation and Ottawa sand, corresponding to an adsorption of 0.16 mg of surfactant/g of porous media.

Figure 2 shows a typical model fit of the experimental data. The model matches the data well but tends to overestimate the concentrations in the tailing region of the experiments. In Table 1, the estimated values of the fitted mass-transfer correlation parameters β_0 and β_2 are given for each experiment. Since β_1 was fitted from the ensemble of experimental results, only a single value of this parameter was estimated, rather than for each experiment. The average

values of each correlation parameter and the accompanying 95% confidence intervals over all of the experiments are as follows:

$$\begin{aligned}\beta_0 &= 760 \pm 130 \quad (\text{surfactant concentration} = 1.6\%) \\ \beta_0 &= 390 \pm 20 \quad (\text{surfactant concentration} = 4.0\%) \\ \beta_1 &= 1.04 \pm 0.15 \\ \beta_2 &= 1.15 \pm 0.03\end{aligned}\quad (5)$$

In general, the confidence intervals around the best estimates of the parameters are relatively small, indicating that the uncertainty in the parameter estimates is relatively low. There is a significant difference between the estimated values for β_0 for the two surfactant concentrations, since the confidence intervals about the estimated values for each β_0 do not overlap. The remaining two parameters were not significantly correlated to the surfactant concentration.

The fact that the β_0 parameter decreases with increasing surfactant concentration implies that the apparent mass-transfer rates decrease with increasing surfactant concentration. This result could be explained by the difference between the first-order rate constants found for the two surfactant solutions, where the rate constants decreased with increasing surfactant concentration. It is worth noting that the ratio of the first-order rate constants measured from the batch experiments for the two surfactant solutions, 1.5 to 1 (2.4 min⁻¹ for the 1.6% solution to 1.5 min⁻¹ for the 4.0% solution), is on the order of the ratio of the β_0 parameters, 2.2 to 1 (790 for the 1.6% solution to 360 for 4.0% solution).

Grimberg et al. (11) also found that the mass-transfer coefficients for a phenanthrene–nonionic surfactant system decreased with surfactant concentration. They attributed this result to increases in micelle volume with increasing surfactant concentrations, which would decrease the diffusivity of micelles toward the NAPL–aqueous phase interface. An alternative explanation is that, since surfactants tend to accumulate near the NAPL–aqueous phase interface, their presence could alter diffusion rates near the interface. At higher surfactant concentrations, diffusion rates may be reduced by the presence of greater numbers of surfactant monomers and micelles at or near the interface, resulting in lower mass-transfer rates. Both of these explanations are based on variations in diffusivity, which would suggest that diffusivities for the surfactant solutions should be measured and incorporated into the Sherwood number calculations and by introducing the Schmidt number ($Sc = \rho/\mu D^*$) into the mass-transfer correlation, allowing for a nonlinear relationship between the mass-transfer rate coefficient and diffusivity.

3.3. Comparison of Mass Transfer Rate Coefficients and Correlations. The value of β_1 , the parameter associated with Re , is high when compared to values obtained in experiments where NAPL was dissolved with water only (without surfactant), which are typically in the range of 0.60–0.75 (e.g., 7, 17). Apparently, the highest value reported for an exponential coefficient associated with pore velocity in NAPL dissolution experiments is 0.9 (21). The higher value of β_1 found here for surfactant-enhanced solubilization may indicate that the diffusional resistances are more sensitive to variations in velocity when surfactants are present. In addition, the configuration of the discrete NAPL blobs or ganglia is likely to be different when surfactants are present, since the NAPL–aqueous phase interfacial tension is expected to be at least an order of magnitude lower than in the freshwater case. With lower interfacial tensions, a larger number of smaller blobs would be expected, which could result in a greater

dependence of mass-transfer rates on the diffusion limitations near the NAPL–aqueous phase interface.

Nelson and Galloway (22) derived an expression for mass-transfer from dense systems of fine particles where Sh was linearly related to Re , implying $\beta_1 = 1$. This result was obtained for the limiting case where $Re \rightarrow 0$. Derivations of the mass-transfer rates for multiregion conceptual models have indicated that mass-transfer rates depend on pore velocities raised to the order of unity or greater, implying $\beta_1 \geq 1$ (cf. 12). Both the work of Nelson and Galloway (22) and Soerens et al. (12) indicate that β_1 may depend on Re . An alternative explanation for high values of β_1 is that aqueous-phase bypassing may be occurring, where the aqueous phase is in contact with both uncontaminated, or NAPL-free, regions and regions containing NAPL. Dissolution fingers, which could contribute to bypassing, are more likely to form when the equilibrium concentration is higher (23), as is the case with surfactant-enhanced solubilization, relative to freshwater dissolution.

The average value of β_2 found here is higher than values typically found for freshwater dissolution (7, 17) and found for cosolvent-enhanced solubilization (18) when correlations similar to (eq 3) were fitted to experimental data. A value of β_2 as high as 1.08 was estimated by Imhoff et al. (24) for freshwater solubilization for relatively nonuniform porous media. The higher value of β_2 found here could be explained by the fact that the porous medium used in the experiments reported here was less uniform than for previously reported NAPL solubilization experiments. The magnitude of the β_2 parameter has been related to the degree of porous media uniformity, where β_2 increases with decreasing uniformity (18). An alternative explanation for variations in β_2 might be that the configuration of the NAPL, including the interfacial area available for mass-transfer, is significantly different in the presence of surfactants, due to reduction of the aqueous phase–NAPL interfacial tension.

The mass-transfer rate coefficients found here for a NAPL–surfactant system can be compared to the rate coefficients found for NAPL–freshwater systems. For a pore velocity of $v = 0.007$ cm/s and a NAPL volumetric fraction of $\theta_n = 0.03$, the mass-transfer rate coefficient calculated from eqs 3 and 5 is 430 day⁻¹. Using the correlation given in Imhoff et al. (24) for TCE dissolution in freshwater and the same pore velocity and NAPL volumetric fraction, a range of mass-transfer rate coefficients from 3000 to 15 000 day⁻¹ is obtained. The mass-transfer rate coefficients obtained here for surfactant-enhanced solubilization for TCE are at least an order of magnitude lower than those obtained for freshwater dissolution. This result is consistent with the findings of Pennell et al. (2), where divergences from equilibrium concentrations were from 2 to 7 times greater for surfactant systems when compared to freshwater systems. A potential explanation for this phenomenon is that the accumulation of surfactants near the NAPL–aqueous phase interface could retard the diffusion of either NAPL dissolved in the aqueous phase or micelles containing NAPL. This explanation can be further related to the previous observation that the mass-transfer rate apparently decreases with increasing surfactant concentration.

The mass-transfer rate coefficients and correlations determined here can be compared to findings from investigations of other NAPL–surfactant systems. The mass-transfer rate correlations determined by Ji and Brusseau (5), Mason and Kueper (4), and Abriola et al. (3) are listed in Table 2. Figure 4 compares the mass-transfer rate coefficients produced from the Ji and Brusseau (5) and Mason and Kueper (4) correlations and the correlations determined here, as a function of θ_n . The results shown in Figure 4 were produced for a pore velocity of 0.007 cm/s and an initial NAPL volumetric fraction (θ_n^0) of 0.067, which are the experimental

TABLE 2. Mass-Transfer Correlations Determined for Other NAPL–Surfactant Systems^a

NAPL–surfactant system	mass-transfer correlation	ref
TCE–sodium dodecyl sulfate	$Sh = \frac{d_p^2}{D^*} \beta_0^* \left(\frac{\theta_n}{\theta_n^0} \right)^{\beta_2}$ $\beta_0^* = 6840 \text{ day}^{-1}$ $\beta_2 = 2.5$	Ji and Brusseau (1998)
PCE–nonylphenol ethoxylate/ phosphate ester of a nonylphenol ethoxylate	$Sh = \beta_0 Re^{\beta_1} \left[\left(1 - \frac{\theta_n}{\phi} \right)^3 - \left(1 - \frac{\theta_n}{\phi} \right)^5 \right]$ $\beta_0 = 13.79 - 20.67$ $\beta_1 = 0.202 - 0.368$	Mason and Kueper (1996)
dodecane– polyoxyethylene (20) sorbitan monooleate	$Sh = 0.00315 + \beta_0 Re^{\beta_1}$ $\beta_0 = 0.0049$ $\beta_1 = 0.192$	Abriola et al. (1993)

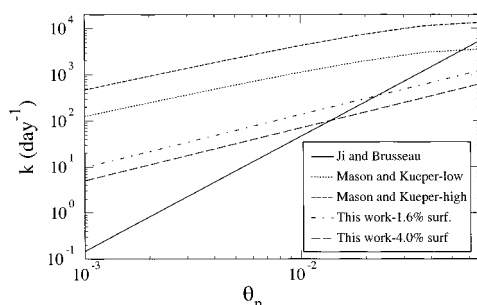
^a ϕ = porosity.

FIGURE 4. Comparison of the mass-transfer rate coefficient correlations, where the mass-transfer rate coefficient is plotted with respect to NAPL volumetric fraction. The “Mason and Kueper-low” curve was produced with $\beta_0 = 20.67$ and $\beta_1 = 0.368$, corresponding to the experiments conducted with a 0.3 gradient. The “Mason and Kueper-high” curve was produced with $\beta_0 = 34.6$ and $\beta_1 = 0.202$, corresponding to the experiments conducted with a 0.1 gradient.

parameters used by Ji and Brusseau (5) to generate their correlation.

There is little agreement among the three correlations in terms of the magnitude of the estimated mass-transfer rate coefficients. The lack of agreement could be attributed to differences in the experimental procedures or to differences in the physical and chemical properties of the NAPL–surfactant system. The NAPL–surfactant system used in the Mason and Kueper (4) experiments apparently exhibits significant chemical nonequilibrium, since more than 1000 min was required for equilibrium concentrations to be reached in batch experiments. This result would suggest that the mass-transfer rates should be lower for the Mason and Kueper (4) NAPL–surfactant system; however, the mass-transfer rates for Mason and Kueper (4) shown in Figure 4 are higher than the rates for the NAPL–surfactant system used here. The higher mass-transfer rates for Mason and Kueper (4) could be explained by the fact that their experiments involved upward flooding of a NAPL pool, where the contact between the NAPL and the surfactant solution would be expected to be much greater than in systems with a residual NAPL.

On the other hand, the dependence of the mass-transfer rate on θ_n is similar for the Mason and Kueper (4) correlations and the correlations found here. The agreement is evidenced by the similarity in slopes for these correlations in Figure 4, at least up to about $\theta_n = 0.03$. The $\beta_2 = 2.5$ value found for the Ji and Brusseau (5) correlation results in a significantly higher slope and a much lower estimated mass-transfer rate coefficient at lower NAPL volumetric fractions. It is surprising that Ji and Brusseau (5) obtained such a high value for β_2 ,

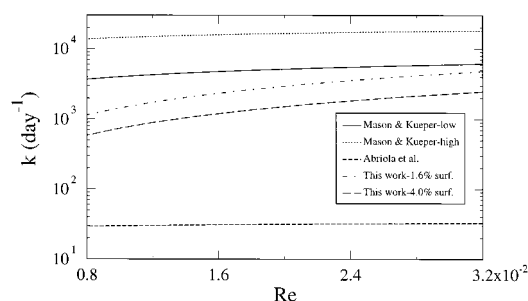


FIGURE 5. Comparison of the mass-transfer rate coefficient correlations, where the mass-transfer rate coefficient is plotted with respect to Reynolds number. The “Mason and Kueper-low” curve was produced with $\beta_0 = 20.67$ and $\beta_1 = 0.368$, corresponding to the experiments conducted with a 0.3 gradient. The “Mason and Kueper-high” curve was produced with $\beta_0 = 34.6$ and $\beta_1 = 0.202$, corresponding to the experiments conducted with a 0.1 gradient.

given that the degree of tailing in their experimental data is similar to that observed in the experiments reported here.

The dependence of the mass-transfer rate coefficient on Re is compared in Figure 5 for the Mason and Kueper (4) correlations, the Abriola et al. (3) correlation, and the correlations found here. The mass-transfer rate coefficients were calculated for $\theta_n = 0.06$, which is the average value of θ_n used to generate the Abriola et al. (3) correlation. Again, there is little agreement between the correlations in terms of the magnitudes of mass-transfer rate coefficients. The rate coefficients estimated with the Abriola et al. (3) correlation are especially low, due to the lower values for both the β_0 and β_1 parameters. The values of the β_1 parameters found for the Mason and Kueper (4) and Abriola et al. (3) correlations are significantly lower than the parameter value estimated here. This difference is likely due to variations in the physical and chemical properties among the NAPL–surfactant systems.

On the basis of both general principles and qualitative observations with many surfactant solutions (13), one would expect large differences in the behavior of surfactants with widely different molecular structures and charges. Properties such as cmc, micelle aggregation number and size, surfactant monomer and micelle diffusion coefficient, and viscosity of the aqueous surfactant solutions vary widely among surfactant chemical compositions (14). For example, aqueous-phase viscosities can vary more than an order of magnitude when only the surfactant molecular structure is changed (27). These properties are sensitive to the electrolyte environment in the case of anionic surfactants, to temperature in the case of nonionic surfactants, and to the cosolvent concentration for both anionic and nonionic surfactants. All of these differences would be expected to have a significant effect on

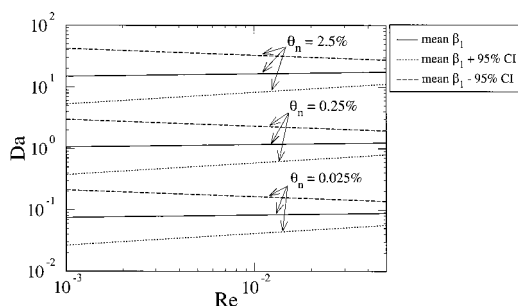


FIGURE 6. Damkohler number (Da) versus Reynolds number (Re) for mean, mean plus one 95% confidence interval ($\beta_1 = 1.19$), and mean minus one 95% confidence interval for β_1 and for $\theta_n = 2.5\%$, $\theta_n = 0.25\%$, and $\theta_n = 0.025\%$.

the rate of mass-transfer and the time required for surfactant solutions to reach equilibrium with the NAPL.

3.4. Implications. The magnitude of the Damkohler number, $Da = kL/v$, where L is a characteristic length, is an indication of how near a system is to equilibrium, where higher values of Da indicate equilibrium or near-equilibrium conditions. Equations 3 and 5 can be substituted for k in the Damkohler number expression, by rearranging eq 3 to solve for k . The significance of the β_1 parameter, the exponent associated with the Reynolds number, is assessed in Figure 6, where Da is plotted against Re . The Damkohler number estimates shown in Figure 6 were calculated with the parameter values for the 1.6% surfactant concentration, a characteristic length of 1 m, and a range of NAPL volumetric fractions. The results are shown using the mean ($\beta_1 = 1.04$), the mean plus one 95% confidence interval ($\beta_1 = 1.19$), and the mean minus one 95% confidence interval ($\beta_1 = 0.89$).

The results shown in Figure 6 for the mean value of β_1 indicate that Da is relatively insensitive to Re , implying that the degree of nonequilibrium does not change with residence time. This surprising result can be explained by the fact that, since the pore velocity, v , is found in the Reynolds number term in eq 3 and the mean value of β_1 is slightly greater than unity, Da is proportional to v raised to a small, positive power. Thus, as the pore velocity increases, Da changes only slightly. The results for the mean plus one 95% confidence interval indicate that Da increases with decreasing residence time, which is an even less intuitive result. However, the results for the mean minus one 95% confidence interval show that the degree of nonequilibrium increases with decreasing residence time, since, in this case, the power associated with the pore velocity in the $Da-v$ relationship is negative.

Regardless of the $Da-v$ relationship, the values of Da in Figure 6 for $\theta_n = 2.5\%$ (ranging from about 5 to 40) indicate that the system is at equilibrium ($C/C_s \geq 0.99$ at $x = L$) at this relatively high NAPL volumetric fraction for all values of Re . Values of C/C_s are calculated using a simple relationship that neglects dispersion: $C/C_s(x=L) = 1 - \exp(-Da)$. However, for lower volumetric fractions, nonequilibrium conditions can occur. For $\theta_n = 0.25\%$, the values of Da range from 0.33 to 4.6, corresponding to a range of $C/C_s = 0.28$ to 0.90 at $x = L$. For $\theta_n = 0.025\%$, the values of Da range from 0.023 to 0.14, corresponding to a range of $C/C_s = 0.032$ to 0.13 at $x = L$. The sensitivity of the degree of nonequilibrium to the NAPL volumetric fraction illustrates the significance of the value of β_2 . The decrease in mass-transfer rates as the NAPL volumetric fraction decreases is quite sensitive to this parameter (25). Higher values of the β_2 parameter will increase the severity of tailing at low NAPL volumetric fractions.

The relationship between Da and v has very important implications for designing surfactant floods; however, the confidence intervals on β_1 could allow a wide range of conclusions with regard to the selection of flooding rates in

relation to the attainment of equilibrium. Since the range of pore velocities used to develop the mass-transfer correlation was relatively narrow (0.0059–0.021 cm/s), caution should be used when interpreting the results concerning the relationship between attainment of equilibrium conditions and pore velocities. Furthermore, the correlation reported here was developed for NAPL volumetric fractions of 4.0% and less. Extrapolation to higher NAPL volumetric fractions, especially levels above residual, could lead to erroneous results.

The practical implication of nonequilibrium mass-transfer between NAPL and surfactant solution is that removing a specified mass of NAPL will require more time than that calculated assuming equilibrium. Equilibrium assumptions should be used with caution because this approach will significantly underestimate the amount of time and mass of surfactant required to solubilize a given volume of NAPL. More research is needed to determine the underlying physical and chemical mechanisms that control mass-transfer rates in NAPL-surfactant systems, since it may be possible to manipulate physical and chemical conditions to improve surfactant flood efficiencies. For example, larger-scale physically-based mechanisms, such as bypassing, may be more important than small-scale mass-transfer limitations. In this case, the use of mobility control agents during the surfactant flood may increase the apparent mass-transfer rates, thus increasing the efficiency of the flood. Dwarakanath et al. (26) found that effluent concentrations of TCE increased by about 25% when polymers were used in a surfactant flood of a packed laboratory column. Furthermore, it makes sense to investigate and apply surfactant formulations that reach chemical equilibrium with a given NAPL quickly, such as the case with the NAPL-surfactant system used here, as evidenced by the batch and early column experimental results.

Acknowledgments

We gratefully acknowledge the support of Varadarajan Dwarakanath in the development of the experimental procedures used in this work and his insightful comments on our manuscript. This work was supported by Grant Agreement R825405-0-01 from the U.S. Environmental Protection Agency Office of Research and Development. Although the information in this document has been funded wholly or in part by the U.S. EPA, it does not necessarily reflect the views of the Agency, and no official endorsement should be inferred.

Literature Cited

- (1) Pennell, K. D.; Abriola, L. M.; Weber, W. J., Jr. Surfactant-Enhanced Solubilization of Residual Dodecane in Soil Columns. 1: Experimental Investigation. *Environ. Sci. Technol.* **1993**, 27 (12), 2332–2340.
- (2) Pennell, K. D.; Jin, M.; Abriola, L. M.; Pope, G. Surfactant Enhanced Remediation of Soil Columns Contaminated by Residual Tetrachloroethylene. *J. Contam. Hydrol.* **1994**, 16, 35–53.
- (3) Abriola, L. M.; Dekker, T. J.; Pennell, K. D. Surfactant-Enhanced Solubilization of Residual Dodecane in Soil Columns. 2: Mathematical Modeling. *Environ. Sci. Technol.* **1993**, 27 (12), 2341–2351.
- (4) Mason, A. R.; Kueper, B. H. Numerical Simulation of Surfactant Flooding to Remove Pooled DNAPL from Porous Media. *Environ. Sci. Technol.* **1996**, 30 (11), 3205–3215.
- (5) Ji, W.; Brusseau, M. L. A General Mathematical Model for Chemical-Enhanced Flushing of Soil Contaminated by Organic Compounds. *Water Resour. Res.* **1998**, 34 (7), 1635–1648.
- (6) Fountain, J. C.; Starr, R. C.; Middleton, T.; Beikirch, M.; Taylor, C.; Hodge, D. A Controlled Field Test of Surfactant-Enhanced Aquifer Remediation. *Groundwater* **1996**, 34 (5), 910–916.
- (7) Miller, C. T.; Poirier-McNeill, M. M.; Mayer, A. S. Dissolution of Trapped Nonaqueous Phase Liquids: Mass Transfer Characteristics. *Water Resour. Res.* **1990**, 26 (11), 2783–2796.

- (8) Carroll, B. J. The Kinetics of Solubilization of Nonpolar Oils by Nonionic Surfactant Systems. *J. Colloid Interface Sci.* **1981**, 79 (1), 126–135.
- (9) Ward, A. J. Kinetics of Solubilization in Surfactant-Based Systems. In *Solubilization in Surfactant Aggregates*; Surfactant Science Series 55; Christian, S. D., Scamehorn, J. F., Eds.; Marcel Dekker: New York, 1995; pp 237–273.
- (10) Chen, B.-H.; Miller, C. A.; Garrett, P. R. Rates of Solubilization of Triolein into Nonionic Surfactant Solutions. *Colloids Surf.* **1997**, A128, 129–143.
- (11) Grimberg, S. J.; Nagel, J.; Aitken, M. D. Kinetics of Phenanthrene Dissolution into Water in the Presence of Nonionic Surfactants. *Environ. Sci. Technol.* **1995**, 29 (6), 1480–1487.
- (12) Soerens, T. J.; Sabatini, D. A.; Harwell, J. H. Effects of Flow Bypassing and Nonuniform NAPL Distribution on the Mass Transfer Characteristics of NAPL Dissolution. *Water Resour. Res.* **1998**, 34 (7), 1657–1673.
- (13) Dwarakanath, V. Characterization and Remediation of Aquifers Contaminated by Nonaqueous Phase Liquids Using Partitioning Tracers and Surfactants. Ph.D. Thesis, The University of Texas at Austin, 1997.
- (14) Bourrel, M.; Schechter, R. S. *Microemulsions and Related Systems*, Marcel Dekker: New York, 1988; p 30.
- (15) Kostarelos, K.; Pope, G. A.; Rouse, B. A.; Shook, G. M. A New Concept: The Use of Neutrally-Buoyant Microemulsions for DNAPL Remediation. *J. Contam. Hydrol.* **1998**, 4 (34), 383–397.
- (16) Jin, M.; Delshad, M. R.; Dwarakanath, V.; McKinney, D. C.; Pope, G. A.; Sepehrnoori, K.; Tilburg, C.; Jackson, R. E. Partitioning Tracer Test For Detection, Estimation and Remediation Performance Assessment of Subsurface Nonaqueous-phase Liquids. *Water Resour. Res.* **1995**, 31 (5), 1201–1212.
- (17) Powers, S. E.; Abriola, L. M.; Weber, W. J. An Experimental Investigation of Nonaqueous Phase Liquid Dissolution in Saturated Subsurface Systems-Transient Mass Transfer Rates. *Water Resour. Res.* **1994**, 30 (2), 321–332.
- (18) Imhoff, P. T.; Gleyzer, S. N.; McBride, J. F.; Vancho, L. A.; Okuda, I.; Miller, C. T. Cosolvent-Enhanced Remediation of Residual Dense Nonaqueous Phase Liquids: Experimental Investigation. *Environ. Sci. Technol.* **1995**, 29 (8), 1966–1976.
- (19) Efron, B.; Gong, G. A Leisurely Look at the Bootstrap, the Jackknife, and Cross-Validation. *Am. Stat.* **1983**, 37 (1), 36–48.
- (20) Mendenhall, W.; Scheaffer, R. L.; Wackerly, D. D. *Mathematical Statistics with Applications*; PWS Publishers: Boston, 1986; 750 pp.
- (21) Baldwin, C. A.; Gladden, L. F. NMR Imaging of Nonaqueous-Phase Liquid Dissolution in a Porous Medium. *Am. Inst. Chem. Eng. J.* **1996**, 42 (5), 1341–1349.
- (22) Nelson, P. A.; Galloway, T. R. Particle-to-Fluid Heat and Mass Transfer in Dense Systems of Fine Particles. *Chem. Eng. Sci.* **1975**, 30, 1–6.
- (23) Imhoff, P. T.; Miller, C. T. Dissolution Fingering During the Dissolution of Nonaqueous Phase Liquids in Saturated Media I. Model Predictions. *Water Resour. Res.* **1996**, 32 (7), 1919–1928.
- (24) Imhoff, P. T.; Arthur, M. H.; Miller, C. T. Complete Dissolution of Trichloroethylene in Saturated Porous Media. *Environ. Sci. Technol.* **1998**, 32 (16), 2417–2424.
- (25) Mayer, A. S.; Miller, C. T. The Influence of Mass Transfer Characteristics and Porous Media Heterogeneity on Nonaqueous Phase Liquid Dissolution. *Water Resour. Res.* **1996**, 32 (6), 1551–1567.
- (26) Dwarakanath, V.; Kostarelos, K.; Pope, G. A.; Shotts, D.; Wade, W. H. Anionic Surfactant Remediation of Soil Columns Contaminated by Nonaqueous Phase Liquids. *J. Contam. Hydrol.* **1999**, 38 (4), 465–488.
- (27) Weerasooriya, V.; Yeh, S. L.; Pope, G. A. Integrated Demonstration of Surfactant-Enhanced Aquifer Remediation and Reuse. *ACS Symp. Ser. Surfact.-Based Sep.: Recent Adv.* **1998**.

Received for review December 28, 1998. Revised manuscript received June 9, 1999. Accepted June 18, 1999.

ES9813515